Simulation of myelinated neuron with focus on conduction speed and changeable excitability

Pengfei Chen Sung Min Kim

Abstract

In this paper we focus on the two particular properties of myelinated neuron, the increased conduction speed and changeable excitability. First we implemented myelinated neuron using NEURON simulator and verified in simulation the previously known two properties mentioned above. Next we tried to identify in simulation which channels were responsible for changeable excitability. Finally we verified that the structure of dendrites could also affect the changeable excitability.

1 Introduction

Myelin sheath is a protective coat around the axon of a neuron and acts as an insulator to the electrical signal that is conducted down the axon as a neuron fires. This increases the conduction speed of action potential and thus is a critical factor in maintaining the proper communication within the complex nervous system. For example in multiple sclerosis, which is characterized by disrupted myelination, has devastating symptoms including physical, mental and sometimes psychiatric problems. Another important property of myelination is that it causes changeable excitability after action potential. Changeable excitability is the result of three factors during the recovery cycle: 1.inactivation of fast sodium channel, 2.depolarizing afterpotential(DAP) and 3.hyperpolarizing afterpotential(HAP). Previous studies have found that in the DAP region the threshold of subsequent firing is smaller and in the HAP region the threshold of subsequent firing is larger[1]. Another study[2] has found that the shape and the pattern of action potential is influenced by dendritic structure which suggests that changeable excitability could be caused not only by myelination but also by dendritic structure.

In this study we tried to build a model that simulates myelination and use this model to verify in simulation the increased conduction speed and changeable excitability. For changeable excitability we first checked whether the particular shape of DAP and HAP was observed. Then we tried to experiment with input signal of different magnitude to check whether the threshold of subsequent firing changed. To identify which channels are responsible for DAP and HAP, we shut down four different types of channels - fast Na^+, persistent Na^+, slow K^+ and leak channel - one by one and saw how the shape of afterpotential was affected. Lastly, we tried to replace myelinated axon with unmyelinated axon in neurons with complicated dendritic structure to exclude any possible effect of myelination and thus to see more clearly the effect of dendritic structure on firing pattern and shape of action potential.

2 Methods

We constructed two neurons with simple dendrites but with myelinated and unmyelinated axon, respectively, to compare their properties. Then we constructed two neurons with complex dendrites but with myelinated and unmyelinated axon, respectively.

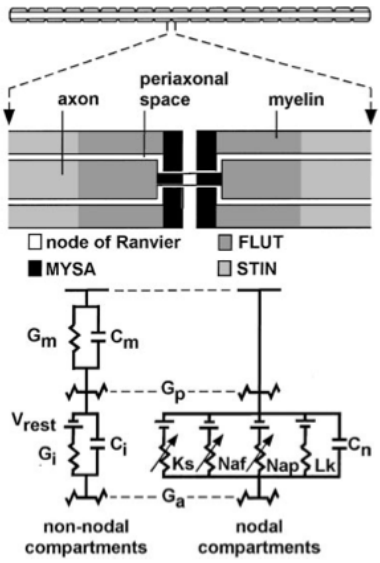

Figure 1: Multi-compartment double cable model of a mammalian axon. The internodal segments were represented by a double cable structure of linear conductances with an explicit representaion of the myelin sheath and the internodal axolemma [1].

2.1 Neuron with myelinated axon and simple dendrites

To simulate the myelinated axon, we use the double cable model in [1]. Their models of mammalian nerve fibers were developed with explicit representations of the nodes of Ranvier, paranodal, and internodal sections of the axon, as well as a finite impedance myelin sheath (Fig. 1). The models were implemented in NEURON v4.3 [3] and solved using backward Euler implicit integration with a time step of $0.001-0.005$ ms.

All the geometric parameters we use are given in Table 1 in [1], where we use the set of parameters with fiber diameter $10.0\mu m$. All the electrical parameters are given in Table 2 in [1].

2.1.1 Fiber geometry

The model consists of 21 nodes of Raniver separated by 20 internodes. Each internodal section of the model consisted of 2 paranodal myelin attachment segments (MYSA), 2 paranodal main segments (FLUT), and 6 internodal segments (STIN)(Fig. 1).

A soma was attached at the end of the myelinated axon with diameter $100\mu m$ and length $100\mu m$. Three dendrites were attached at the opposite end of the soma. Each dendrite was $25\mu m$ in diameter and $500\mu m$ in length.

2.1.2 Membrane dynamics

The nodes consisted of the parallel combination of nonlinear fast Na^+ , persistent Na^+ , and slow K^+ conductances, a linear leakage conductance, and the membrane capacitance. The time and voltage dependence of each gating parameter (ω) is given by

$$\tau_\omega = 1/(\alpha_\omega + \beta_\omega) \quad (1)$$

$$d\omega/dt = \alpha_\omega(1-\omega) - \beta_\omega\omega \quad (2)$$

The time course and magnitude of the activation and inactivation parameters used in the simulations are given below. Based on the work of [4], a singel-channel conductance of 15 and 8pS were used for the fast Na^+ and slow K^+ channels, respectively. We used a density of 2,000 channels/μm^2 [5] for the nodal fast Na^+ channels, resulting in a g_{Naf} of 3.0 S/cm^2. We used a density of 100 channels/μm^2 [6] for the nodal slow K^+ channels resulting in a g_{Ks} of 0.08 S/cm^2. The membrane

dynamics were derived to be representative of neural excitation at 36°C.
Fast Na^+ current

$$I_{Naf} = g_{Naf} * m^3 * h * (V_m - E_{Na}) \tag{3}$$
$$\alpha_m = [6.57 * (V_m + 20.4)]/\{1 - e^{[-(V_m+20.4)/10.3]}\} \tag{4}$$
$$\beta_m = 0.304 * [-(V_m + 25.7)]/\{1 - e^{[(V_m+25.7)/9.16]}\} \tag{5}$$
$$\alpha_h = 0.34 * [-(V_m + 114)]/\{1 - e^{[(V_m+114)/11]}\} \tag{6}$$
$$\beta_h = 12.6/1 + e^{[-(V_m+31.8)/13.4]} \tag{7}$$

Persistent Na^+ current

$$I_{Nap} = g_{Nap} * p^3 * (V - m - E_{Na}) \tag{8}$$
$$\alpha_p = [0.0353 * (V_m + 27)]/\{1 - e^{[-(V_m+27)/10.2]}\} \tag{9}$$
$$\beta_p = 0.000883 * [-(V_m + 34)]/\{1 - e^{[(V_m+34)/10]}\} \tag{10}$$

Slow K^+ current

$$I_{Ks} = g_{Ks} * s * (V_m - E_K) \tag{11}$$
$$\alpha_s = 0.3/\{1 + e^{[(v_m+53)/-5]}\} \tag{12}$$
$$\beta_s = 0.03/\{1 + e^{[(v_m+90)/-1]}\} \tag{13}$$

Leakage current

$$I_{LK} = g_{LK} * (V_m - E_{LK}) \tag{14}$$

For the soma we used Hodgkin-Huxley model implemented in NEURON and set $E_{Na} = 50mV$, $E_K = -90mV$ and $E_{LK} = -90mV$, which were the same with the values applied in the membrane dynamics in the myelinated axon. But the channels were different. Hodgkin-Huxley model contains fast Na^+ current, fast K^+ current and leakage current. Another difference is that the Hodgkin-Huxley model in NEURON was supposed to work at 6.3°C. We used the Hodgkin-Huxley model because we didn't find a whole set of parameters for a soma with the same membrane dynamics working at the same temperature as the axon in [1].

For the dendrites we used passive mechanism implemented in NEURON and set the reversal potential E_{pas} to be -80mV, which was the same as the rest potential of the membrane.

The results turned out to be fine(See next section). Action potential could be initiated in the dendrites and pass through the soma into the myelinated or unmyelinated axon.

2.2 Neuron with unmyelinated axon and simple dendrites

A neuron with unmyelinated axon was construced. The unmyelinated axon had the the same length and diameter as the myelinated one. The structure of the soma and dendrites between this and the last neuron are the same.

We used Hodgkin-Huxley model implemented in NEURON with default paramters in both axon and soma. Passive mechanism implemented in NEURON with default parameters is used for dendrites.

2.3 Neuron with myelinated axon and complex dendrites

To investigate how the configuration of dendrites affects the afterpotential, we used the model in [2], where they simulated neurons with identical channel distributions but four different dendritic morphology(See Fig. 6 a, b, c, d).

Standard compartmental modelling techniques were used to simulate spatially extended neurons with passive electrical structure, four voltage-dependent currents: fast Na^+, I_{Na}; fast K^+, I_{Kv}; slow non-inactivating K^+, I_{Km}; and high-voltage activated Ca^{2+}-dependent current, I_{Ca} and one Ca^{2+}-dependent current, I_{KCa}. All currents were calculated using conventional Hodgkin-Huxley-style kinetics with an integration time step of 250ps.

As we use their code in this part, all the geometry of the neuron and membrane dynamics are the same as in [2].

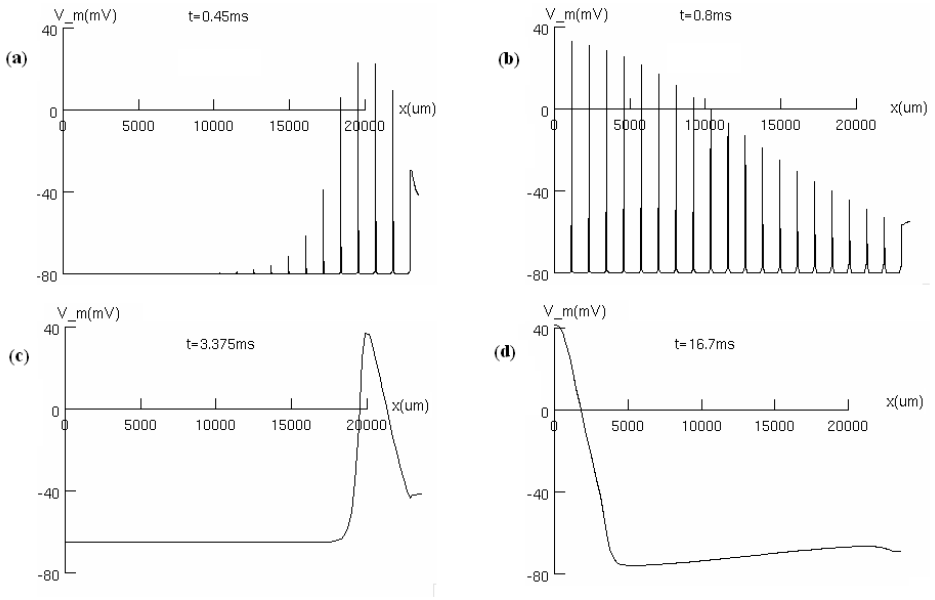

Figure 2: Comparison of the conduction speed of action potentials in myelinated versus unmyelinated neurons. (a),(b) It took 0.8-0.45=0.35 ms for action potential to travel 20,000 μm along the myelinated axon. (c),(d) It took 16.7-3.375 = 13.325 ms for action potential to travel 20,000 μm along the unmyelinated axon.

2.4 Neuron with unmyelinated axon and complex dendrites

Since the axon of the neuron in [2] is myelinated, we would like to see what would happen if we change it to an unmyelinated one. So we replace the original myelinated axon with an unmyelinated one with the same diameter and length. The new axon has passive electrical structure, fast Na^+ and fast K^+ currents. The parameter for each of those currents are still the same as in [2].

3 Results

3.1 Conduction speed

We attached soma and simple dendrites to the myelinated axon model in [1] to get the first neuron. Then we replaced the myelinated axon with an unmyelinated one to construct another neuron. An alpha synapse was initiated at the same position of the dendrites of those two neurons. The propagation of the action potential was compared.

Our simulation showed that conduction speed was much faster in myelinated neuron (Fig. 2). This is because the regeneration of action potential, which is the major time consuming process, occurs all the way along the unmyelinated axon whereas it occurs only at the node of myelinated axon. Although this comparison is not exact in that the two neurons are made of different types of channel mechanisms, it still clearly showed how minimized number of regeneration process of action potential reduces time needed to travel a given distance.

3.2 Changeable axonal excitability

We put a current clamp in the middle of the axon and measure the membrane voltage at the same position. The distinctive shape of DAP and HAP was observed exclusively in myelinated neuron and was well in accord with experimental data (Fig. 3). Theses shapes are responsible for changeable excitability when more than one firing is subsequently triggered during the recovery cycle of preceeding firing. The recovery cycle after action potential spike can be divided into three regions: 1. Na channel inactivation, 2. DAP, and 3. HAP.

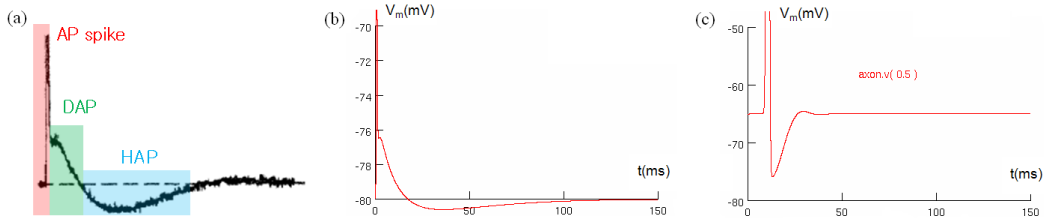

Figure 3: Shape of action potential. (a) Experimental data[1].(b) Simulated data of myelinated neuron. (c) Simulated data of unmyelinated neuron.

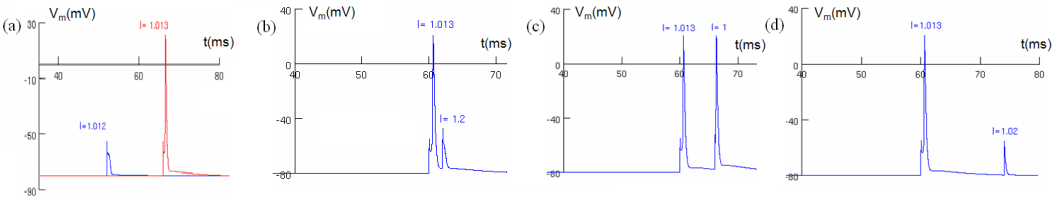

Figure 4: Experiments to verify changeable excitability. (a) The approximate threshold current I_{th0} was found. 1.012 nA $< I_{th0} <$ 1.013 nA (b) $I_{th} >$ 1.2 nA $> I_{th0}$ due to inactivation of fast Na^+. (c) $I_{th} <$ 1.0 nA $< I_{th0}$ due to DAP. (d) $I_{th} >$ 1.02 nA $> I_{th0}$ due to HAP.

We first measured the thresdhold of single firing as a baseline(Fig. 4a). Then we measured threshold of second firing in two consecutive firing event. When the second firing was in the fast Na^+ channel inactivation region the second action potential was not generated even with supranormal threshold which means increased threshold (Fig. 4b). When the second firing was in DAP region subnormal threshold was enough to trigger second firing which means decreased threshold (Fig. 4c). When the second firing was in HAP region supranormal threhold was not enough to trigger second firing which means increased threshold (Fig. 4d). All together, these experiments show excitability changes due to DAP and HAP as a result of myelination.

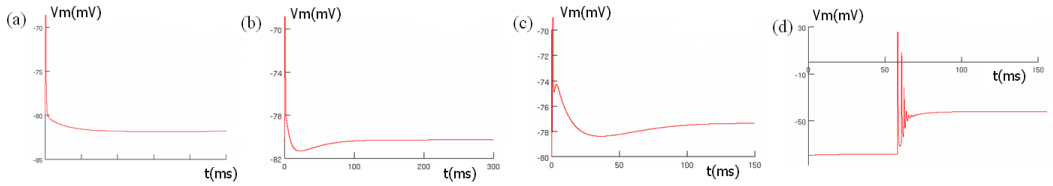

Figure 5: Channels were shut down one kind by one kind to check which kind is responsible for DAP or HAP. (a) Fast Na^+ channels shutdown: No DAP or HAP, and larger current was needed to initiate an action potential. (b) Persistent Na^+ channels shutdown: No DAP but AHP remains. (c) Leakage current shutdown: DAP remains, reduced HAP. (d) Slow K^+ channels shutdown: failure of recovery back to the original rest potential.

3.3 Channels that cause DAP and HAP

Next we investigated which channels are responsible for the formation of DAP or HAP. The occurence of DAP or HAP altered when different types of channels were shutdown (Fig. 5). Fast Na^+ channel seemed to play the most significant role in the occurence of DAP and HAP since both disappeared when Naf was shutdown (Fig. 5a). Linear leakage channel seemed to have the least influence on DAP and HAP since neither changed much when Lk was shut down (Fig. 5c). Persistent Na^+ channel seemed to cause DAP as well because only DAP disappeared after shutdown (Fig. 5b).

Slow K^+ channel was shown to be responsible for repolarization back to original resting membrane potential (Fig. 5d).

3.4 Effect of dendritic structure

So far we have seen that myelination can cause DAP and HAP which lead to changeable excitability. Some other studies have shown that dendritic structure could also affect the shape and pattern of action potential [2] (Fig. 6a,b,c,d).

In their study the axon is myelinated. To see the effect of dendritic structure more clearly excluding any possible interference of myelination on the shape of action potential we replaced the original myelinated axon in already established model [2] with unmyelinated axon and ran the simulation again. Our results are shown in Fig. 7, which are very close to the results in [2](Fig. 6). This means that myelination is not a necessary condition for generation of afterpotentials.

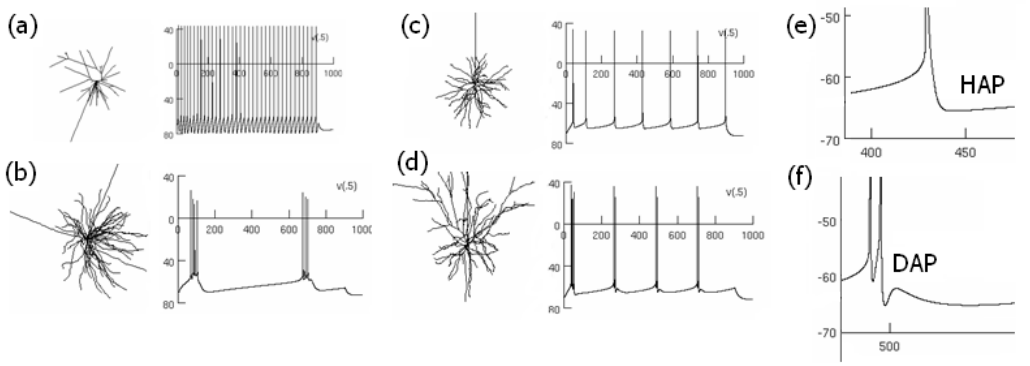

Figure 6: Effect of dendritic structure on the shape of action potential in myelinated neuron. Digital reconstructions of dendritic arborizations of neurons from rat somatosensory cortex (a) and cat visual cortex(b-d). (a) Layer 3 aspiny stellate, (b) Layer 4 spiny stellate, (c) Layer 3 pyramid, (d) Layer 5 pyramid. Different dendritic structure caused different firing pattern and shape. (e) Magnification of (c) where HAP appeared. (f) Magnification of (d) where DAP appeared.

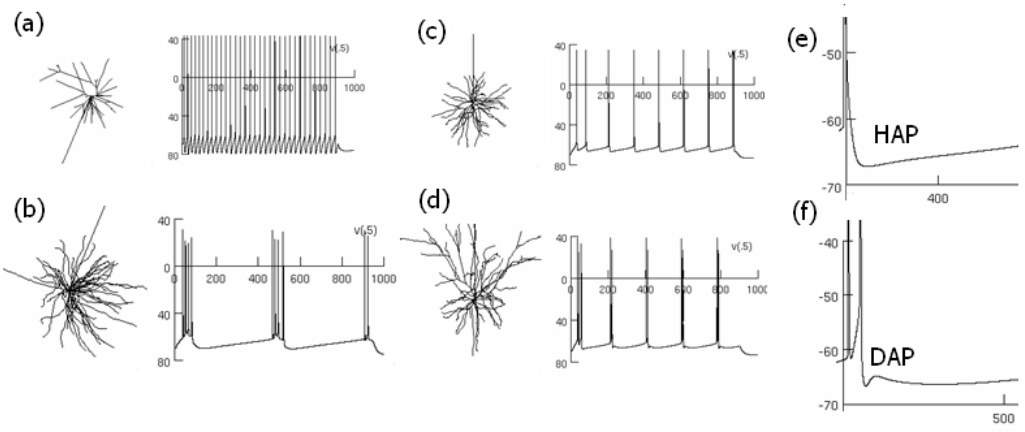

Figure 7: Effect of dendritic structure on the shape of action potential in unmyelinated neuron. (a)(b)(c)(d) Neurons with same dendrites configuration as Fig. 6, but the axon is umyelinated. Spiking patterns and shape of afterpotentials are similar with Fig. 6.

Moreover DAP and HAP was observed without myelination but with some particular dendritic structure (Fig. 7e,f). This suggests that DAP and HAP can be caused solely by dendritic structure. This also strongly implies that changeable excitability can also result from dendritic structure as well

independent of myelination. According to [2], the two parameters that matter in shaping firing behaviour are the ratio of axo-somatic area to dendritic membrane area and the coupling resistance between axo-somatic and dendritic compartments.

4 Conclusion

In this study, we have shown that myelination and dendritic structure are responsible for the occurence of DAP and HAP which are in turn responsible for altered threshold of subsequent action potential. We have quantatatively shown that the threshold is different depending on the timing of subsequent firing, depending on whether it lies in the DAP or HAP region. DAP decreases threshold whereas HAP increases threshold. In case of myelination, the channels are concentrated at the node region and we have identified in simulation that the fast sodium channel plays the most significant role in the formation of DAP and HAP and potassium leak channel showed least significant role. We also have shown that the conduction speed is much faster in myelinated axon because of the vertically insulated myelin which minimizes the occurence of time-consuming regeneration of action potential.

For future study it would be insteresting to expand the model toward the network of neurons and investigate any emergent properties that result from changeable excitability and interactions between multiple neurons.

5 References

[1] McINTYRE, C.C., Richardson, A.G. & Grill, W.M. (2002) Modeling the Excitability of Mammalian Nerve Fibers:Influence of Afterpotentials on the Recovery Cycle. *J Neurophsiol* 87:995-1006

[2] Mainen, Z.F. & Sejnowski, T.J. (1996) Influence of dendritic structure on firing pattern in model neocortical neurons. *Nature* 382:363-366

[3] Hines, M.L., & Carnevale, N.T. (1997) The NEURON simulation environment. *Neural Comput* 9:1179-1209

[4] Schwarz, J.R., Reid, G. & Bostock, H. (1995) Action potentials and membrane currents in the human node of Ranvier. *Pflugers Arch* 430:283-292

[5] Waxman, S.G., & Ritchie, J.M. (1993) Molecular dissection of the myelinated axon. *Ann Neurol* 33:121-136

[6] Safronov, B.V., Kampe, K. & Vogel, W. (1993) Single voltage-dependent potassium channels in rat peripheral nerve membrane. *J Physiol (Lond)* 460:675-691